Materials Research Proceedings **10** (2019) 107-113 doi: http://dx.doi.org/10.21741/9781644900031-15

Microstructural Design of Ni-base Superalloys by Hot Isostatic Pressing

Benjamin Ruttert [1,a *], Inmaculada Lopez-Galilea [1], Lais Mujica Roncery [2] and Werner Theisen [1]

[1] Lehrstuhl Werkstofftechnik, Ruhr-Universität Bochum, 44801 Bochum, Germany

[2] Grupo de Investigación en Materiales Siderúrgicos e INCITEMA, Universidad Pedagógica y Tecnológica de Colombia, Boyacá, Colombia

[a] benjamin.ruttert@.rub.de

Keywords: HIP, Microstructure, Ni-base Superalloy, Porosity, Rejuvenation

Abstract. Single-crystal Ni-base superalloys (SXs) are used as a first-stage blade material in high-pressure turbines for aero engines or in stationary gas turbines. They operate at temperatures close to their melting point where they have to withstand mechanical and chemical degradation. Casting and extensive solution heat-treatments of such blades introduce porosity that can only be reduced by hot isostatic pressing (HIP). Recent developments in HIP plant technology enable simultaneous HIP-heat-treatments due to rapid quenching at the end of such treatments. This work gives an overview of the opportunities that such a unique HIP offers for the solution heat-treatment of conventionally cast SXs or directionally solidified Ni-base superalloys fabricated by selective electron beam melting (SEBM). The influence of temperature, pressure, and cooling method on the evolution of the γ/γ'-morphology and on the pore shrinkage is investigated. The cooling method has a strong impact on the γ'-particle size and shape whereas the combination of temperature and pressure during the HIP-treatment mainly influences porosity reduction. In a final approach a HIP treatment is satisfactorily used to fully re-establish the γ/γ'-microstructure after high-temperature creep degradation.

Introduction

SXs are used as a first-stage blade material in modern gas turbines [1]. Their complex composition results in large dendrite arm spacings during the slow Bridgman solidification process, with heavy partitioning of alloy elements between dendritic and interdendritic regions as well as the formation of large cast pores in interdendritic regions. The presence of porosity reduces the material strength and ductility and results in scattering of the mechanical properties. Pores act as crack initiation sites and promote crack propagation, leading to premature rupture of the components [2-3]. Therefore, it is important not only to reduce the segregation by a heat-treatment (solution annealing and aging), but also to reduce the porosity generated during casting and solution annealing by means of HIP. Modern HIP units can provide fast quenching rates that help in designing the desired microstructures starting from material states that feature internal pores, undesirable precipitates, and chemical segregation. The simultaneous application of a high isostatic pressure and a high temperature can eliminate pores by a combination of elementary processes that involve plastic deformation, creep, and diffusion bonding and also simultaneously remove chemical heterogeneities of the alloy. The possibility of controlling the cooling rate after HIP to a certain degree (from quenching to slow cooling) enables establishment of a desired final γ/γ' microstructure at the end of such an implemented HIP-heat-treatment [4]. Consequently, the combination of HIP and quenching enables integration of the required homogenization of the

Materials Research Proceedings **10** (2019) 107-113 doi: http://dx.doi.org/10.21741/9781644900031-15

superalloys within the HIP-process, thus resulting in one processing step [5]. The present contribution intends to give an overview of the influence of HIP parameters such as temperature, pressure, and cooling rate of modern HIP units on porosity reduction as well as on the evolution of the γ/γ'-microstructure of cast SX as wells as additively manufactured Ni-base superalloys. Since SX turbine blades operate under harsh service conditions (high temperatures and stresses), time-dependent microstructural changes occur that degrade the microstructure and thus the lifetime of the blades: namely rafting and the formation and growth of cavities. The high costs of SX components has led to an increased interest in extending their service live by various repair and rejuvenation procedures [6]. Lastly, a short approach is made in this work to rejuvenate the crept microstructure by an appropriate HIP-rejuvenation.

Materials and methods

In this work, the ERBO/1 SX is investigated. It is a CMSX-4 type of alloy with a specific heat-treatment [7]. ERBO/1 is used in three different states: as-cast (ERBO/1A), after solution annealing in a laboratory vacuum furnace (ERBO/1B) and after conventional solutioning and subsequent precipitation hardening (ERBO/1C). All details regarding the chemical composition, homogeneity, and microstructural details have been described elsewhere [7]. All specimens used in this work were precisely oriented in the <100> direction by combining the Laue technique with electro discharge machining [7]. The specimens for scanning electron microscopy (SEM) were examined perpendicularly to the solidification direction for microstructural characterization at the dendrite core and parallel to the solidification direction for porosity quantification. For the porosity measurement, SEM back-scattered electron panorama montages (magnification: 500x), covering a total area of 3 mm x 3 mm were taken. The porosity was determined in the (100)-plane, parallel to the dendrite growth direction. The healing of pores is described, by determining the total measured pore area of ERBO/1(A, B or C) divided by the remaining pores after the different HIP treatments. Quantitative microstructural analysis of the porosity and the γ/γ'-microstructure was supported by the software Image J. High-resolution dilatometry was carried out to determine the γ′-solvus temperature [5]. HIP was performed in two different HIP facilities. The first one of type QIH-9 URQ, from Quintus Technologies, allows ultra-rapid quenching (up to 2000 K/min), as well as very low cooling rates with controlled cooling conditions. The second one of type QIH-9, is able to reach cooling rates of up to 200 K/min. All HIP experiments were carried out in molybdenum furnaces under an inert Ar atmosphere.

Results and discussion

The main characteristic parameters of an as-processed SX microstructure are its γ/γ'-phase morphology and the cast porosity. The temperature and hydrostatic pressure parameters of HIP govern the kinetics of pore shrinkage during the process. However, the cooling rate in combination with the HIP temperature down to room temperature govern the evolution of the γ/γ' microstructure. In order to reduce porosity by a HIP treatment, it is important to apply a temperature that is higher than the γ'-solvus temperature because pressure-driven material flow is fast only if the soft γ-phase is present. At temperatures below $T_{\gamma'\text{-solvus}}$, γ'-particles are present that strengthen the γ-matrix. The resulting increase in creep resistance makes compaction associated with pore shrinkage more difficult. Fig. 1 shows how the HIP temperature and HIP pressure affect the healing of pores. The porosity values of the homogenized material in the laboratory ERBO/1B (without HIP) are 0.365 area% pores, 48 pores/mm^2 and 10 µm average pore diameter [5].

Materials Research Proceedings **10** (2019) 107-113 doi: http://dx.doi.org/10.21741/9781644900031-15

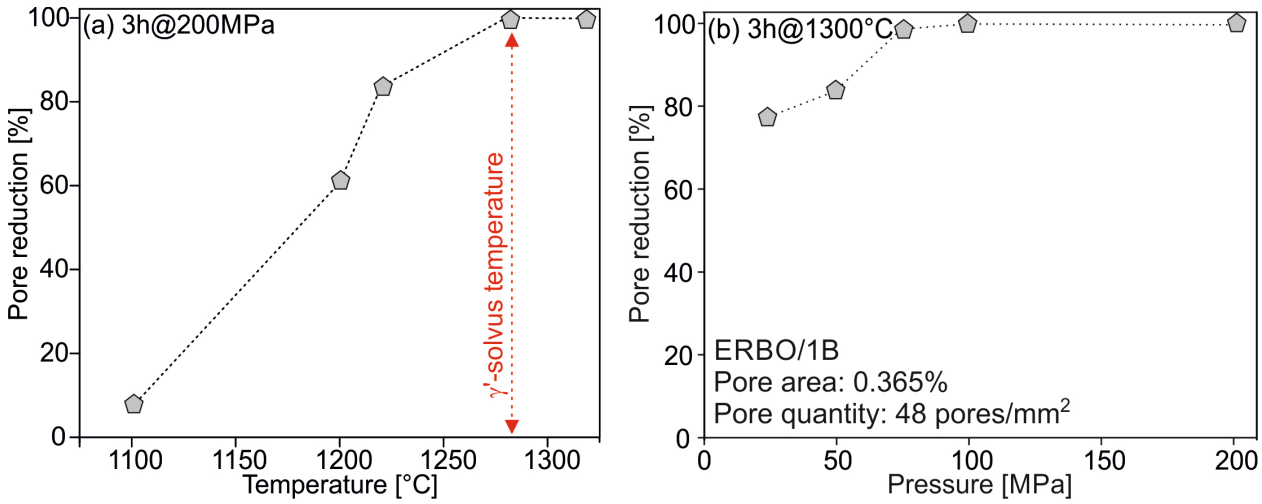

Fig. 1. Influence of HIP parameters on pore healing. (a) Effect of HIP temperature for 3h HIP exposure and a pressure of 200 MPa on conventionally heat-treated ERBO/1C. (b) Effect of HIP pressure at a temperature of 1300°C and 3h exposure on homogenized ERBO/1B. The porosity values of conventionally heat-treated ERBO/1B are given as a reference. Figure modified from ref. [5]

Fig. 1a shows the results of HIP experiments in which a HIP pressure of 200 MPa was applied for 3 hours at different HIP temperatures. The $T_{\gamma'\text{-solvus}}$ was determined to be 1285°C using a high-resolution calorimetry method (shown as a dashed vertical red line in Fig. 1a) [5]. Fig. 1a shows that full porosity reduction can only be achieved at temperatures above the $T_{\gamma'\text{-solvus}}$ and also shows that 1100°C is not a sufficiently high HIP temperature for eliminating as-cast porosity. Higher temperatures favor pore shrinkage because material flow due to high-temperature plasticity is faster (mechanical aspect) and because the diffusion coefficients of alloy elements increase (kinetic aspect). Fid. 1b shows the effect of HIP pressure on porosity reduction for HIP treatments performed at 1300°C for three hours and also shows that porosity reduction becomes more effective when the HIP pressure increases up to 75 MPa, taking the overall pore area of ERBO/1B into account. However, from this pressure value onwards, a further pressure increase does not further accelerate pore healing. It is interesting to note that even low HIP pressures such as 25 and 50 MPa achieve porosity reductions of 77 and 99%, respectively. The fact that higher pressures result in more effective porosity reduction results from the fact that higher pressures represent higher driving forces for plasticity controlled compaction. Typical porosity values after HIPing at 1300°C for 3h at 100 MPa pressure are 0.001 area% pores, 1 pores/mm^2 and 2.6 µm average pore diameter [5]. The features of the γ/γ' microstructure strongly depend on the cooling rate after the isothermal HIP treatment. This has been studied for the alloy ERBO/1B. Different cooling rates were applied after 3h isothermal HIP treatments at 100 MPa and 1300°C. After HIP, three different cooling rates were applied: fast, intermediate, and slow. By approximating the cooling curves as straight lines in the temperature interval between 1300 and 800°C, these three cooling rates can be approximated as 30 K/s (fast), 1 K/s (intermediate) and 0.3 K/s (slow). It was found that the cooling rates after HIP did not affect the porosity. However, they have a strong influence on the γ/γ'-microstructure, as shown in Fig. 2a to 2c. Decreasing cooling rates result in an increasing particle size and decreasing particle number fractions. Faster cooling rates are associated with smaller particles in which smaller elastic strain energies are less effective in enforcing cuboidal shapes. Whereas the effect of

Materials Research Proceedings **10** (2019) 107-113 doi: http://dx.doi.org/10.21741/9781644900031-15

cooling rate on the particle structure directly after cooling is more or less as expected, it is worth noticing that different cooling rates effect the γ/γ' microstructures, even when two-stage post-HIP heat-treatments of 1140°C for 4h and 870°C for 16h at atmospheric pressure are applied (see Fig. 2d to 2f). The results shown in Fig. 2d to 2f clarify that these additional heat-treatments result in a controlled type of particle coarsening which establishes the final microstructure. When the systems starts with a larger γ' particle size, it also has larger γ'-particle sizes after the additional heat-treatment steps, as can be seen by comparing Fig. 2d and 2f. Post-HIP annealing heat-treatments also result in a higher degree of regularity of the γ/γ'-microstructure.

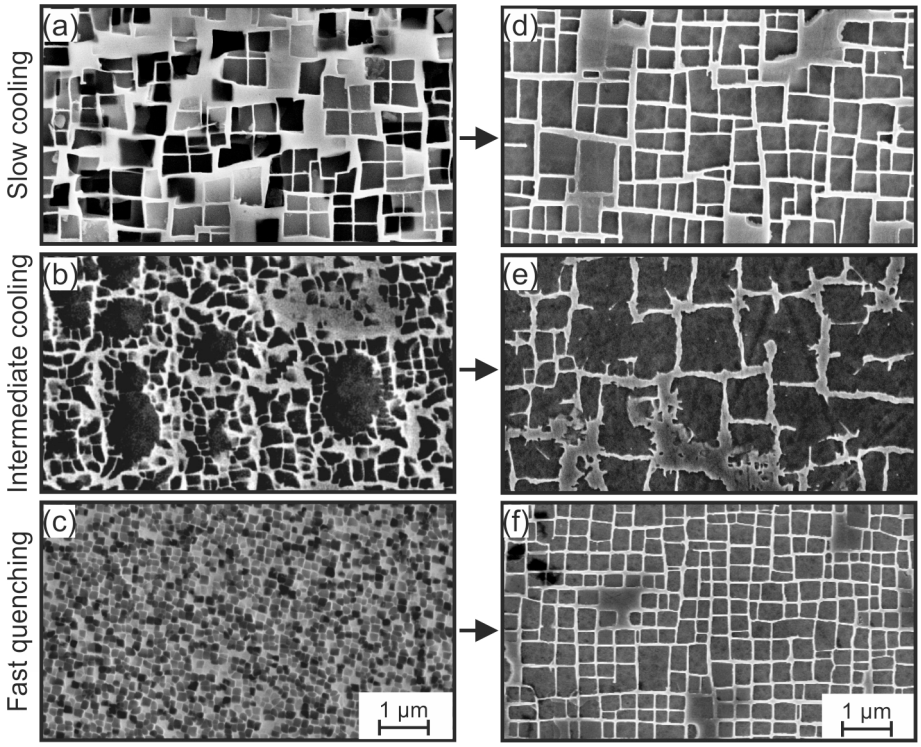

Fig. 2. SEM micrographs illustrating the effect of the cooling rate on the microstructure that terminates the HIP cycle at 100 MPa pressure. (a)-(c) Microstructures after different cooling rates. (d)-(f) Microstructures after cooling and an additional two step aging.

Electron-beam melting was used to build cylindrical, columnar-grained parts from pre-alloyed and atomized CMSX-4 powder [8]. The microstructure of such parts is very fine and the dendrite arm spacing is several orders of magnitude finer than that of cast parts. Therefore, the required homogenization time of such parts to reduce elemental partitioning can be significantly shortened. A first approach was made in this work, in which homogenization of a SEBM part was transferred into a novel HIP with quenching capability (see Fig. 3a). SEBM parts in the as-built condition still exhibit microstructural heterogeneities such as small pores (Fig. 3b) and small-scale elemental partitioning as shown qualitatively in the Re-element mapping in Fig. 3c. The results of Fig. 3d and 3e demonstrate that only a few minutes of isothermal holding time in combination with a moderate heating rate are sufficient to almost completely shrink the porosity (Fig. 3d) and to dissolve the elemental partitioning (Fig.3e). Rapid quenching at the end of the holding step leads to small and uniformly distributed γ'–precipitates, as described previously in

Materials Research Proceedings **10** (2019) 107-113 doi: http://dx.doi.org/10.21741/9781644900031-15

this section. Additionally, due to the layerwise manufacturing during SEBM (in-situ heat-treatment), the resulting γ'–precipitate size is a function of the distance from the bottom to the top surface of the manufactured parts [8]. At the HIP-homogenization temperature, however, the γ'-size gradient is dissolved first and subsequent rapid quenching produces a fine and uniform γ'-size distribution that is favorable for the following precipitation hardening.

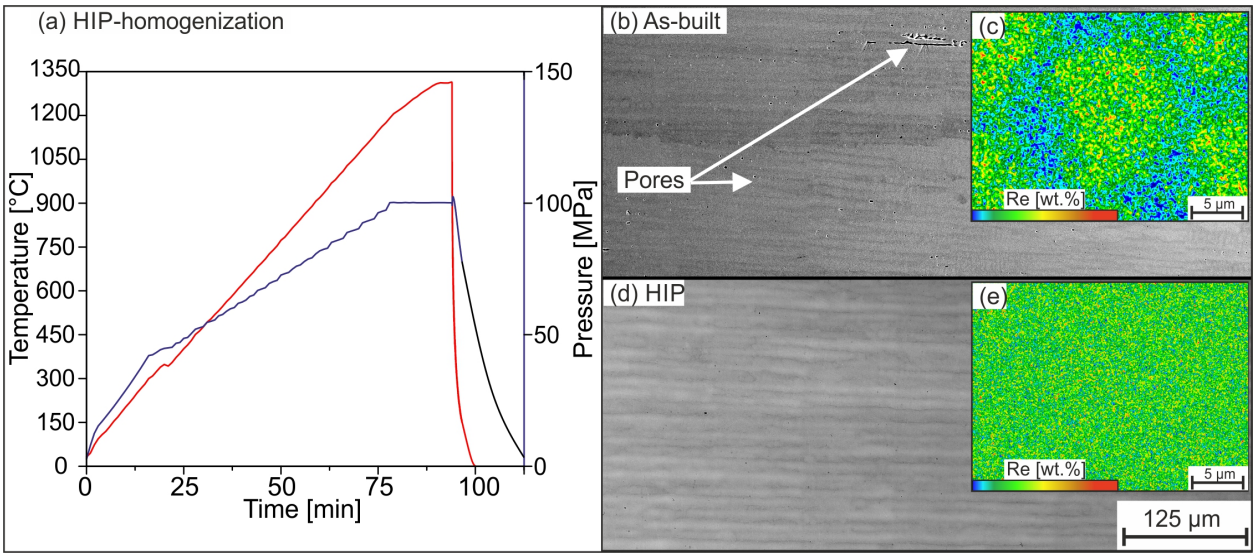

Fig. 3. HIP heat-treatment for the EBM part and SEM micrographs showing the microstructural evolution. (a) HIP treatment at a pressure of 100 MPa and 30 min HIP exposure. (b) Microstructure in the as-built longitudinal section, showing pores, and (c) showing an EDS element mapping for Re. (d) and (e) show the corresponding microstructures after the HIP treatment.

At least a first step has been made to explore whether the γ/γ'-microstructure of the initial material state can be re-established by HIP after high-temperature creep deformation. A conventionally heat-treated ERBO/1C specimen was creep deformed at 1050°C and 160 MPa to a final strain of 5%. The microstructure of this material state was investigated in the SEM. Fig. 4a shows an SEM micrograph of the rafted microstructure after high-temperature creep deformation. The specimen was then subjected to the HIP-rejuvenation treatment shown in Fig. 4b. After 4h of isothermal HIP with rapid quenching (fast cooling, section I), subsequent precipitation hardening (4 hours at 1140°C and 16 hours at 870°C) was performed in a laboratory furnace under an Ar atmosphere at atmospheric pressure. The microstructural evolution of the crept and subsequently rejuvenated material states are compared in Fig. 4a and 4c, respectively. It can be clearly seen that the rafts have disappeared and that a fine and uniform γ/γ'-microstructure was re-established. Further work is required to fully exploit the potential of a HIP rejuvenation treatment. The effect of rejuvenation on porosity, dislocations, recrystallization, on the presence/absence of TCP phases, and lastly on additional creep life must be investigated carefully.

Summary and conclusions

The present work investigates the effect of a novel HIP treatment on the microstructure of an as-cast / as-built, as-cast and heat-treated, and a pre-crept SX of type ERBO 1 (CMSX 4 family). It was shown that HIP treatments can heal porosity. In order to optimize HIP-parameters, temperatures must be higher than the γ'-solvus temperature and pressures consequently higher

Materials Research Proceedings **10** (2019) 107-113 doi: http://dx.doi.org/10.21741/9781644900031-15

than 75 MPa. However, the material's porosity is not affected by the cooling rates after isothermal HIP treatments. In contrast, the cooling rates have a strong influence on the γ/γ'-microstructure. Faster cooling rates result in finer microstructures, directly after HIPing as well as after a subsequent precipitation hardening. A HIP rejuvenation treatment has been shown to restore a fine and regular γ/γ'-microstructure after initial high-temperature creep deformation.

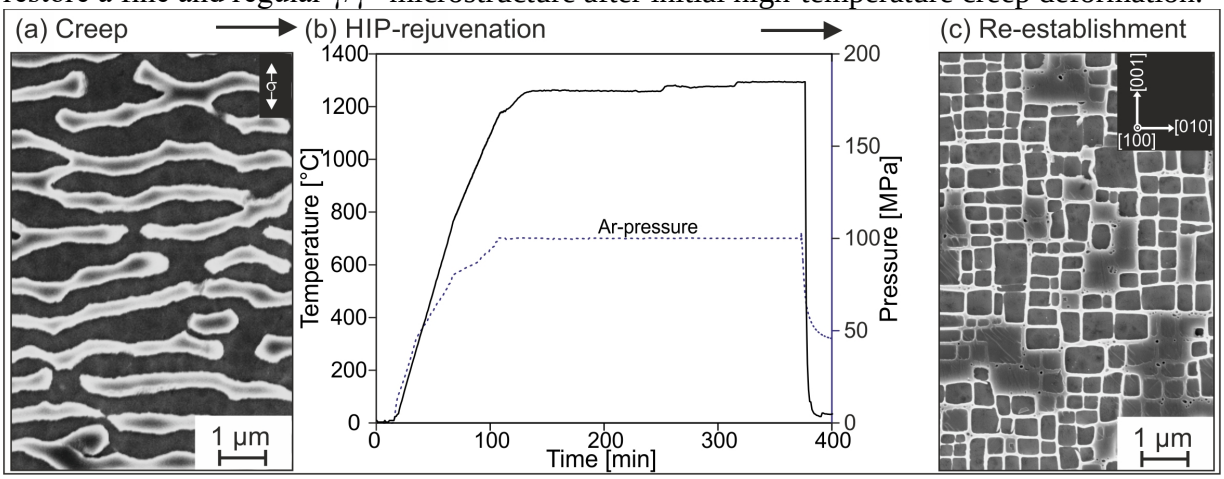

Fig. 4. SEM micrographs showing the effect of HIP-rejuvenation on the microstructure after creep. (a) Topological inversion, and (b) temperature vs time and pressure vs time histories during the rejuvenation. At the end of isothermal HIP exposure: fast quenching. (c) Re-established microstructure.

Acknowledgements

The authors acknowledge funding by the Deutsche Forschungsgemeinschaft (DFG) via the collaborative research center SFB/TR-103 through project B4 (BR, ILG, LMR, WT). Assistance from D. Bürger, P. Wollgramm and G. Eggeler from project A1 for providing the creep specimen and M. Ramsperger and C. Körner from project B2 for providing the EBM parts is gratefully acknowledged.

References

[1] G.W. Meetham, The Development of Gas Turbine Materials, UK, London, (1981). https://doi.org/10.1007/978-94-009-8111-9

[2] A. Epishin, T. Link, Mechanisms of high-temperature creep of nickel-based superalloys under low applied stresses, Philos. Mag. A. 84 (2004) 1979-2000. https://doi.org/10.1080/14786430410001663240

[3] G. Mälzer, R.W. Hayes, T. Mack, G. Eggeler, Miniature Specimen Assessment of Creep of the Single-Crystal Superalloy LEK 94 in the 1000°C Temperature Range, Metall. Mater. Trans. A 38 A (2007) 314-327.

[4] H.V. Atkinson, B.A. Rickinson, Hot Isostatic Processing, UK, Bristol, (1991).

[5] L. Mujica Roncery, I. Lopez-Galilea, B. Ruttert, S. Huth, W. Theisen, Influence of temperature, pressure, and cooling rate during hot isostatic pressing on the microstructure of an SX Ni-base superalloy, Mater. Des. 97 (2016) 544-552. https://doi.org/10.1016/j.matdes.2016.02.051

[6] A. Baldan, Rejuvenation procedures to recover creep properties of nickel-base superalloys by heat treatment and hot isostatic pressing techniques, J. Mater. Sci. 26 (1991) 3409-3421. https://doi.org/10.1007/BF00557126

[7] A.B. Parsa, P. Wollgramm, H. Buck, C. Somsen, A. Kostka, I. Povstugar,P. Choi, D. Raabe, A. Dlouhy, J. Müller, E. Spiecker, K. Demtröder, J. Schreuer, K. Neuking, G. Eggeler, Advanced Scale Bridging Microstructure Analysis of Single Crystal Ni-Base Superalloys; Adv. Eng. Mater. 17 (2015) 216-230. https://doi.org/10.1002/adem.201400136

[8] M. Ramsperger, R.F. Singer, C. Körner, Microstructure of the Nickel-Base Superalloy CMSX-4 Fabricated by Selective Electron Beam Melting, Metall. Mater. Trans. A 47 (2016) 1469–1480. https://doi.org/10.1007/s11661-015-3300-y